r = radial position, cylindrical coordinates, in single free jet
$\mathbf{r}$ = position vector
R = $\equiv D/2$, nozzle radius
R_{ij} = correlation function for fluctuations in the concentrations of components i and j
R_{12} = correlation function for fluctuations in the concentration of material from nozzle streams 1 and 2
s = distance along the jet trajectory, from the virtual origin
U_o = mean discharge velocity at nozzle
U^* = characteristic velocity scale of the interacting jets system, Equation (3)
x, y, z = Cartesian coordinates of the interacting jet system, Figure 1*b*
x_f = virtual origin of the combined jet downstream of the interaction zone

Greek Letters

α = one-half the angle between the jet nozzle axes
Γ = total smoke concentration; $\Gamma \equiv \Gamma_1 + \Gamma_2$
Γ_1, Γ_2 = concentration of smoke from nozzle streams 1 and 2
Γ_i = concentration of smoke from either nozzle stream
$\gamma, \gamma_1, \gamma_2, \gamma_i$ = turbulent fluctuations in $\Gamma, \Gamma_1, \Gamma_2, \Gamma_i$
ϵ = rate of viscous dissipation of turbulent kinetic energy, per unit mass of fluid
κ = $\equiv 2\pi f/\overline{U}_x$, wave number
ν = kinematic viscosity
ρ = density

Subscripts

c = value on the x axis ($y = 0$ and $z = 0$)
i = value when one of the jet nozzle streams is marked with smoke
i, j, k = material of feed streams i, j, and k
0 = value in nozzle stream
1, 2 = smoke from nozzle streams 1 and 2
1, 2, 3 = material of feedstreams 1, 2, and 3

Superscripts

$(\overline{})$ = time-mean value
$(\wedge)$ = root-mean-square value; $\hat{\gamma} \equiv \sqrt{\overline{(\gamma^2)}}$

Dimensionless Parameters

Ma = $\equiv U_o/c$, Mach number
Re = $\equiv U_oD/\nu$, Reynolds number
Sc = $\nu/\mathcal{D}$, Schmidt number for gas in gas

LITERATURE CITED

Baron, T., and E. H. Bollinger, "Mixing of High Velocity Air Jets," Tech. Rept. No. CML-3, Engineering Experimental Station, University of Illinois (1952).

Becker, H. A., H. C. Hottel, and G. C. Williams, Mixing and Flow in Ducted Turbulent Jets," *Ninth Symposium (International) on Combustion,* pp. 7-20, Academic Press New York (1963*a*).

————, "Concentration Intermittency in Jets," *Tenth Symposium (International) on Combustion,* pp. 1253-1263, Academic Press, New York (1965).

————, "Concentration Fluctuations in Ducted Turbulent Jets, *Eleventh Symposium (International) on Combustion,* pp. 791-798, Academic Press, New York (1967*a*).

————, "On the Light Scatter Technique for the Study of Turbulence and Mixing," *J. Fluid Mech.,* **30,** 259-284 (1967*b*).

————, "The Nozzle-Fluid Concentration Field of the Round, Turbulent, Free Jet," *ibid.,* 285-303 (1967*c*).

Becker, H. A., R. E. Rosensweig, and J. R. Gwozdz, "Turbulent Dispersion in a Pipe Flow," *AIChE J.,* **12,** 964-971 (1966).

Booth, B. D., *"Mixing in Intersecting Turbulent Jets,"* M.Sc. thesis, Queen's University, Kingston, Ontario, Canada (1971).

Danckwerts, P. V., "The Definition and Measurement of Some Characteristics of Mixtures, *Appl. Sci. Res.,* A3, 279-296 (1953).

Kirillov, V. A., and B. G. Khudenko, "Calculation of the Direction of the Axis of a Stream Resulting from the Mixing of Turbulent Jets," *J. Eng. Phys.,* **9,** 414-415 (1965).

Makarov, I. S., and B. G. Khudenko, "Mixing of Intersecting Turbulent Jets," *ibid.,* **8,** 304-306 (1965).

Rosensweig, R. E., H. C. Hottel, and G. C. Williams, "Smoke-Scattered Light Measurements of Turbulent Concentration Fluctuations," *Chem. Eng. Sci.,* **15,** 111-129 (1961).

Rummel, K., *Der einfluss des Mischvorganges auf die Verbrennung von Gas and Luft in Feuerungen,* Verlag Stahleisen, Dusseldorf (1937).

Supplementary material has been deposited as Document No. 02679 with the National Auxiliary Publications Service (NAPS), c/o Microfiche Publications, 440 Park Ave. South, New York, N. Y. 10016 and may be obtained for $1.50 for microfiche or $5.00 for photocopies.

Manuscript received February 27, 1975; revision received May 27, and accepted May 28, 1975.

Nonlinear Theory of Free Coating onto a Vertical Surface

The work of Landau and Levich (1942) initiated detailed theoretical and experimental study of the flow of the thin liquid film entrained by a steady withdrawal of a sheet from a bath of liquid. The existing theories, which differ considerably, are all based on linearization of the problem and give single relationships between film thickness T and a capillary number Ca. The present paper demonstrates theoretically that differing physical properties for each liquid result not in a single curve but in a family of curves for T vs. Ca and that the complete set of previous experimental work required and fitted the family of curves. Previous theories could fit only a portion of this experimental data.

The solution requires a nonlinear theory to include inertial terms and two-dimensional flow and thus treat the parameter of liquid physical properties. This is obtained by applying a nonlinear approach based on the direct method of Galerkin. Owing to the nonlinear character of the solution, the new theory has the advantage of accurately determining the shape and size of the upper meniscus profile. Excellent agreement with the complete set of available experimental data is obtained.

M. NABIL ESMAIL

and

RICHARD L. HUMMEL

Department of Chemical Engineering and Applied Chemistry
University of Toronto
Toronto, Ontario

SCOPE

During the past 30 years considerable attention has been given to the theoretical and experimental studies of flow of thin liquid films, entrained from a bath of liquid by continuous steady withdrawal of a sheet. This problem is of considerable practical significance in many industries. Examples include the application of high viscosity liquid films to solid surfaces such as coating of photographic film and paper, the application of polymeric materials to conveyor belts, and lubrication of moving parts of machines in certain aspects.

The formation of these liquid films is characterized by a meniscus thickness decreasing with distance above the bath and eventually approaching a constant thickness region. The resultant constant thickness is a function of the velocity of withdrawal, gravity, and the physical properties of liquid; density, viscosity; and surface tension. In some applications an air flow is used to change this relationship. The meniscus region is characterized at the interface by a stagnation point. The film may be divided about this point into thin and thick menisci. The flow in the thin meniscus is mainly in vertical direction.

The previous theoretical studies of the free coating problem are mainly based on the approach, suggested by Landau and Levich (1942) in their pioneering work. The most significant development in the problem was achieved by White and Tallmadge (1965) who linearized the problem in order to get an analytical but approximate expression for the relationship between the parameters of the problem.

The present paper is concerned with the application of a nonlinear approach (Shkadov, 1967) to the problem of prediction of flow influence on the constant thickness, size, and shape of meniscus profiles in the case of free coating onto a vertical surface. The nonlinear approach employed in this paper has been developed into a general treatment to the problem of wave formation at the interface of thin fluid films (Esmail and Shkadov, 1971, Esmail, 1973). Therefore, it seems to be a powerful approach to the solution of any problem associated with thin fluid films in general. The present paper is confined to the case of free liquid surface. Meanwhile, the nonlinear approach can be applied to cases with directed air flow.

CONCLUSIONS AND SIGNIFICANCE

The relationship between the flow parameters of liquid entrainment from a bath are presented for a wide range of capillary numbers covering flow situations of importance in free coating process equipment. A nonlinear method is applied which permits determining the meniscus shape and size as well as the flow parameters. It is shown (Figures 2, 3, 5) that the consideration of inertial effects splits the solution into a family of curves associated with two parameters, the capillary number and a parameter incorporating physical properties of entrained liquid. The influence of inertial effects on flow parameters and meniscus profiles is significant at a Reynolds number equal to or greater than 0.1. The shapes and sizes of thin meniscus profiles are determined (Figures 4, and 5 and Tables 1 to 5) from the stagnation point up to the constant thickness film. This nonlinear solution holds true up to the appearance of surface waves at Reynolds numbers $\simeq$ 10. Agreement with experimental data (Figure 2, Tables 1 to 5) is excellent. The problem is treated for the first time in a two-dimensional nonlinear approach incorporating the inertial effects. The static meniscus condition, derived by Deryagin and Levi (1964), proves to be the most accurate approximation to the boundary condition at the stagnation point. The one-dimensional linear solution of White and Tallmadge (1965) is an analytical average of the present solution.

MATHEMATICAL MODEL

The steady liquid motion is described by the following system of Navier-Stokes and continuity equations:

$$u\frac{\partial u}{\partial x}+v\frac{\partial u}{\partial y}=-\frac{1}{\rho}\frac{\partial p}{\partial x}+\nu\left(\frac{\partial^2 u}{\partial x^2}+\frac{\partial^2 u}{\partial y^2}\right)-g \tag{1}$$

$$u\frac{\partial v}{\partial x}+v\frac{\partial v}{\partial y}=-\frac{1}{\rho}\frac{\partial p}{\partial y}+\nu\left(\frac{\partial^2 v}{\partial x^2}+\frac{\partial^2 v}{\partial y^2}\right) \tag{2}$$

$$\frac{\partial u}{\partial x}+\frac{\partial v}{\partial y}=0 \tag{3}$$

The coordinates x and y refer to the vertical direction of the sheet and normal direction through the film, respectively (Figure 1). The no slip condition at the moving sheet yields two boundary conditions

$$u=u_0 \quad v=0 \quad \text{for} \quad y=0 \tag{4}$$

The dynamic balance of stresses at the interface including the effect of surface tension may be expressed by

$$\frac{\partial u}{\partial y}+\frac{\partial v}{\partial x}+\frac{2b}{1-b^2}\left(\frac{\partial v}{\partial y}-\frac{\partial u}{\partial x}\right)=0 \tag{5}$$

$$p+\frac{\sigma}{R}+\mu b\left(\frac{\partial u}{\partial y}+\frac{\partial v}{\partial x}\right)-2\mu\frac{\partial v}{\partial y}=p_0 \tag{6}$$

$$b=\frac{da}{dx} \qquad \frac{1}{R}=\frac{db/dx}{(1+b^2)^{3/2}}$$

where $a=a(x)$ is the equation of the free liquid surface. It is necessary to add the kinematic surface condition that expresses the fact that the free surface is a streamline

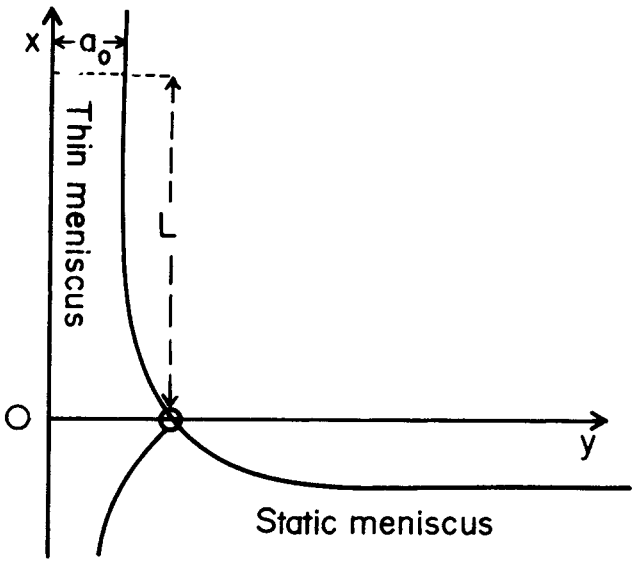

Fig. 1. Definition sketch.

$$Q = \int_0^a u\, dy = \text{const} \tag{7}$$

It is easy to deduce, by using dimensional analysis (Groenveld, 1970), that the relationship between the parameters of the problem should be

$$a_0 \left(\frac{\rho g}{\mu u_0}\right)^{1/2} = f\left(\frac{\rho u_0 a_0}{\mu}, \frac{\mu u_0}{\sigma}\right)$$

or

$$T = f\,(Re, Ca)$$

$$Re = T(Ca\gamma)^{3/2} \quad \gamma = \frac{\sigma}{\rho}\,(g\nu^4)^{-1/3} \tag{8}$$

Only three parameters appear in Equation (8): T, Ca, and γ. The first characterizes the limiting constant film thickness; the second is uniquely associated with the withdrawal speed u_0, and the third incorporates the physical properties of the liquid. In general, the withdrawal speed and the physical properties of liquid, therefore Ca and γ, can be considered known. But for each pair of values for Ca and γ, the solution of the system (1) to (7) gives a family of curves corresponding to various possible film thicknesses. In order to determine the correct film thickness and its associate curve for the particular complete set of conditions, some other physical constraint must be imposed.

PREVIOUS WORK

The initial work of Landau and Levich (1942) regarded the problem as one-dimensional, neglecting the velocities in the meniscus region normal to the moving sheet. Furthermore, the gravity forces were also neglected, limiting the solution to small film thicknesses ($T << 1$, $T^2 \simeq 0$). Landau and Levich introduced the static meniscus condition, considering equilibrium between gravitational and capillary forces in the thick meniscus region:

$$\frac{\sigma \dfrac{d^2a}{dx^2}}{\left[1 + \left(\dfrac{da}{dx}\right)^2\right]^{3/2}} = \rho g x \tag{9}$$

Later, White and Tallmadge (1965) included gravitational forces (terms involving T^2), retaining the one-dimensional assumption. However, in order to apply the static meniscus condition derived by Landau and Levich (1942) and in order to obtain an analytical but approximate expression for the relationship between the parameters of the problem, they linearized the equations, assuming that $a = a_0(1 + \epsilon)$, where ϵ is a small quantity.

As a static meniscus condition, Deryagin and Levi, (1964) introduced a more accurate relation

$$\frac{\sigma}{2\rho g}\left(\frac{d^2a}{dx^2}\right)^2 + \frac{da}{dx} = 1 \tag{10}$$

which may be easily derived for the static meniscus near the top of the free surface.

NONLINEAR APPROACH

The flow and the flow parameters can be described across two horizontal planes. One of these planes is in the constant thickness region. In this region the velocity distribution is parabolic, terminating at the liquid surface at a velocity that is greater than zero:

$$u = \frac{\rho g a_0^2}{\mu}\left[-\frac{y}{a_0} + \frac{1}{2}\left(\frac{y}{a_0}\right)^2\right] + u_0 \tag{11}$$

The flow in this region is constant:

$$Q = \int_0^{a_0} u dy = \frac{a_0 u_0}{3}\,(3 - T^2) \tag{12}$$

Thus, there is an infinite family of solutions for the constant thickness region, but, for each of these, the relationship between the sheet velocity u_0 and the film thickness a_0 is fixed and is in fact determined by the previous regions of the flow. The flow across a horizontal plane through the 'beginning of the constant thickness region' is one of our two boundary conditions.

The second plane across which the flow properties can be described is the horizontal plane through the stagnation point (reported by Groenveld and Van Dortmund, 1970). At the stagnation point, the velocity is precisely zero, and therefore inertial and viscous forces do not exist. If the air is also stagnant, or nearly so, then the pressure at the surface stagnation point is precisely atmospheric.

The second set of boundary conditions would ideally be the velocities through the horizontal plane passing through this stagnation point. According to the suggested nonlinear approach, the width dependence in the flow equations is eliminated by averaging all the unknown functions over the film thickness. Therefore, the solution is sought along the air-liquid interface, and the boundary condition across the horizontal plane passing through the stagnation point reduces to a relationship between the characteristics of the interface curve at the stagnation point and the flow parameters.

These two boundary conditions define the region of concern. Its extent will be called L for subsequent analysis. This region is one of acceleration of the liquid in bulk and along the interface from minimum velocities at the stagnation point to the constant velocities of the constant thickness region. This region determines which of the family solutions apply. Obviously, acceleration terms are required, and therefore a true solution must be nonlinear. The surface boundary condition taken in the present paper is that the air exerts neither variation in pressure nor viscous forces on the surface. However, in industry, air flows are frequently used to change the coating thickness, and for such a problem one must consider pressure and viscous forces exerted on the surface by air.

The velocity distributions across the plane for the stag-

nation point are in fact determined by the flow within the coating chamber which is in turn physically determined by the geometry of the situation. We will consider only one geometry, that is, that of an infinitely deep bath. Thus, at sufficient depth, velocities of concern are constant and equal to that of the motion of the sheet. The region of concern includes the region bounded by the plane through the stagnation point, the sheet, and the streamline terminating in the stagnation point (Figure 1). Here the velocity is greater, and therefore the thickness is less than that of the constant thickness layer. The liquid is decelerated as it approaches the plane of the stagnation point. The deacceleration occurs sharply close to the plane and is transmitted through the streamline terminating in the stagnation point. The flow outside this region and, in particular, the shape of the surface in the thick meniscus region is of no consequence except to the extent that it can be converted accurately into the required boundary condition at the stagnation point. The flow portion, not entrained by the sheet, which forms the thick meniscus, is far slower than the flow entrained from the bath owing to the high viscosity effect. The net difference between the viscous and inertial forces, which is zero on the surface at the stagnation point, remains small on the surface near this point. Since the velocities in the thick meniscus are small, the viscous and inertial forces are small, and the difference between them must be small compared to the forces of gravity and surface tension. Therefore, the thick meniscus may be considered in a static condition up to the stagnation point.

THE DIRECT METHOD OF GALERKIN

The boundary condition chosen for the stagnation point is that of Equation (10). It serves as a solution for the dynamic equations of the flow at the stagnation point by using the assumption of the static condition in the thick meniscus. The significance of Equation (10) is that it preserves the continuity of the slope and curvature of the interface along the entire meniscus. As noted earlier, this equation and Equation (9) by Landau and Levich have been based on an assumption of static condition for the thick meniscus region. This phrasing is unnecessary. In fact, Equation (10) fits the slope and curvature, of the surface for the stagnation point, and whatever else happens in the thick region is not used in this solution.

It is clear from physical considerations of the problem that L is considerably greater than the constant film thickness a_0. Therefore, the condition $n = (a_0)/(L) << 1$ may be introduced. This condition enables estimations of terms in system (1) to (3) and boundary conditions (4) to (7). The introduction of a characteristic vertical velocity $u \sim u_0$ in the continuity equation (3) leads to an expression $v \sim nu_0$ for the characteristic horizontal velocity.

Therefore, system (1) to (3) and boundary conditions (4) to (7) may be considerably simplified, when we neglect terms, estimated as $0(n^2)$ with respect to other terms. As a result, system (1) to (3) will reduce to the following:

$$u\frac{\partial u}{\partial x} + v\frac{\partial u}{\partial y} = -\frac{1}{\rho}\frac{\partial p}{\partial x} + \nu\left(\frac{\partial^2 u}{\partial x^2} + \frac{\partial^2 u}{\partial y^2}\right) - g \tag{13}$$

$$\frac{1}{\rho}\frac{\partial p}{\partial y} = \nu\frac{\partial^2 v}{\partial y^2} \tag{14}$$

$$\frac{\partial u}{\partial x} + \frac{\partial v}{\partial y} = 0 \tag{15}$$

Similarly, the boundary conditions (4) to (7) reduce to

$$u = u_0 \quad v = 0 \quad \text{for} \quad y = 0 \tag{16}$$

$$\frac{\partial u}{\partial y} = 0 \quad (p - p_0) + \frac{\sigma}{R} - 2\mu\frac{\partial v}{\partial y} = 0 \quad \text{for} \quad y = a \tag{17}$$

$$Q = \int_0^a u\,dy = \text{const} \tag{18}$$

The term $\nu(\partial^2 u)/(\partial x^2)$ in Equation (13) was included in spite of its estimation $\sim 0(n^2)$ because it represents the curvatures of flow lines and because calculations reveal its importance especially over the range of low withdrawal speeds.

The equations of the problem (13) to (18) may be replaced by equations integrated with respect to y. This replacement may be considered as the first step in sequential application of the direct method of Galerkin (Shkadov, 1967). This requires the selection of a complete system of functions $W_i(y)$ satisfying the boundary conditions (16) to (18), while the velocity u can be represented as

$$u = \sum_i b_i(x)\ W_i(y) \tag{19}$$

Consequently, the velocity v can be expressed from the continuity equation in the form

$$v = -\sum_i \frac{db_i}{dx}\int_0^y W_i(y)\,dy$$

The application of the direct method will be limited to the first term; therefore, the accuracy obtained may be judged only in comparison with experimental data.

The velocity expression (19) will be assumed to be parabolic in the form

$$u = 3\,U(x)\left[-\frac{y}{a} + \frac{1}{2}\left(\frac{y}{a}\right)^2\right] + u_0 \tag{20}$$

which coincides with the exact solution for the laminar constant thickness film (11), (12).

When we integrate Equation (13) with respect to y from zero to a and introduce the variables

$$h = \frac{a}{a_0} \qquad \xi = \frac{x}{a_0}$$

the system (13) to (15) reduces to the following ordinary differential equation (for details see the appendix)

$$\frac{h^3}{Ca}\frac{d^3h}{d\xi^3} + \left(h^2 - \frac{3}{2}h_s h\right)\frac{d^2h}{d\xi^2} + Re\left(\frac{2}{15}h_s^2 - \frac{h^2}{5}\right)\frac{dh}{d\xi} + 3\,h_s\left(\frac{dh}{d\xi}\right)^2 + (3h - h_s - T^2h^3) = 0 \tag{21}$$

where $h_s = 3 - T^2$.

A similar, but more simplified, equation was first obtained by Landau and Levich (1942) for one-dimensional flow neglecting the effect of gravity:

$$\frac{h^3}{Ca}\frac{d^3h}{d\xi^3} = -(3h - h_s) \tag{22}$$

White and Tallmadge (1965) considered the effect of gravity on one-dimensional flow and obtained

$$\frac{h^3}{Ca}\frac{d^3h}{d\xi^3} = -(3h - h_s - T^2h^3) \tag{23}$$

Only Equation (21) considers two-dimensional flow and

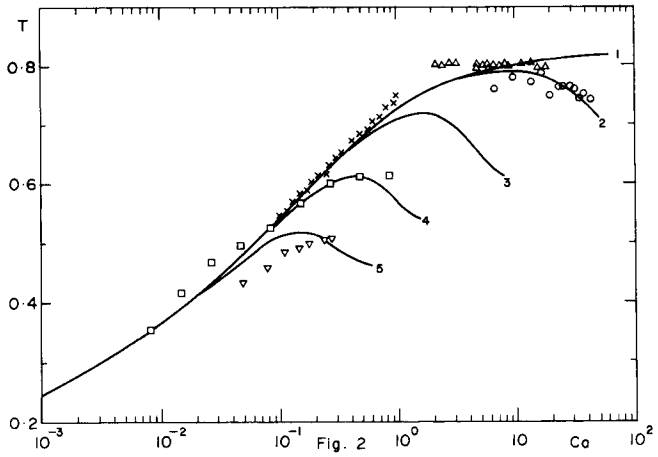

Fig. 2. Comparison of the nonlinear theory with experimental data. Nonlinear theory: 1. $\gamma = 0$; 2. $\gamma = 0.06$; 3. $\gamma = 0.8$; 4. $\gamma = 5$; 5. $\gamma = 18.2$

Experimental data:

- ○ Soroka and Tallmadge, $\gamma = 0.06$.
- △ Spiers et al, lubrication oils.
- × Spiers et al, sugar solutions.
- □ Groenveld, $\gamma = 5$.
- ▽ Gutfinger and Tallmadge, $\gamma = 18.2$.

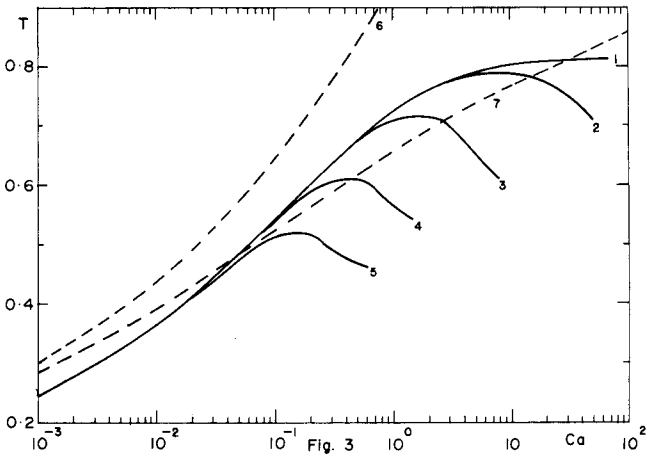

Fig. 3. Comparison of the nonlinear theory with previous theories. Nonlinear theory: 1. $\gamma = 0$; 2. $\gamma = 0.06$; 3. $\gamma = 0.8$; 4. $\gamma = 5$; 5. $\gamma = 18.2$; 6. Landau and Levich; 7. White and Tallmadge.

includes the effect of inertial terms on the characteristics of the problem. Obviously, the term including Reynolds number incorporates the inertial effect, whereas the other first and second derivatives reflect the two-dimensional aspects of the flow.

Equation (21) was integrated over the thin meniscus region, from the beginning of the constant thickness film down to the stagnation point. The starting value procedure of Landau and Levich (1942) provided the initial conditions at the beginning of the constant film thickness:

$$h = 1 + \epsilon \quad h' = \epsilon \quad h'' = \epsilon \tag{24}$$

Equation (21) was solved by numerical integration by using a fourth-order, Runge-Kutta method with the initial conditions (24).

The meniscus thickness of the stagnation point

$$h_s = 3 - T^2 \tag{25}$$

which was derived by Lee and Tallmadge (1973) can be derived with ease by setting u equal to zero at the interface $y = a$ and by using the constant flux condition (12).

By using a simple iteration method, the solution of the numerical integration was adjusted to condition (10) at the stagnation point.

RESULTS AND DISCUSSION

The Parameters of the Flow

As is shown in Figure 2, the solution of the problem for capillary numbers Ca up to a value of 70 comprises a family of curves illustrating the relationship

$$T = f(\gamma, Ca)$$

The parameter γ which creates this family is basically introduced owing to the consideration of inertial terms in the Navier-Stokes equations. Curve 1 in Figure 2 shows the limiting case $\gamma = 0$ for extremely viscous liquids. Each of the other curves corresponds to other value of γ. The branching of these curves begins at a Reynolds number of approximately 0.1. The calculations for each of the selected γ values go up to a Reynolds number of roughly 10. Calculations could not be carried further, which indicates that our assumptions fail for higher Reynolds numbers. As it has been shown (Yih, 1963; Esmail, 1971, 1973), the flow of thin liquid films is in general unstable to certain surface wave disturbances. However, Yih (1963) demonstrated that the flow of thin liquid films is always

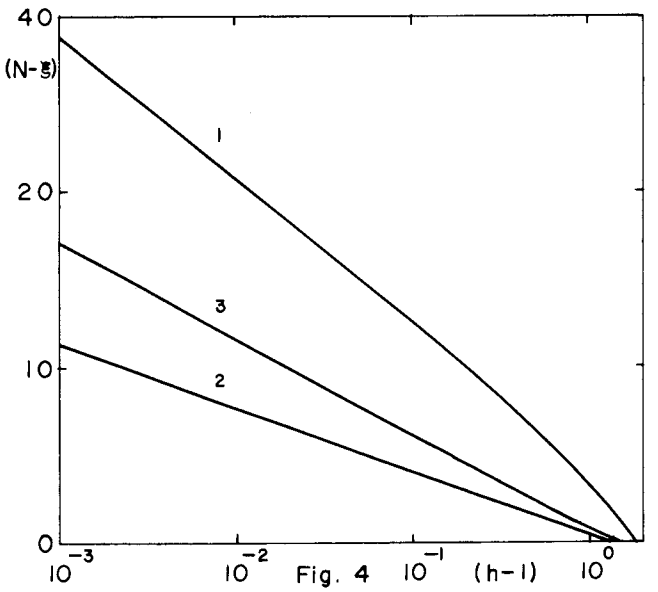

Fig. 4. Semilogarithmic plot of the thin meniscus profiles for $\gamma = 0.06$. 1. Ca = 0.01; 2. Ca = 6.0; 3. Ca = 50.

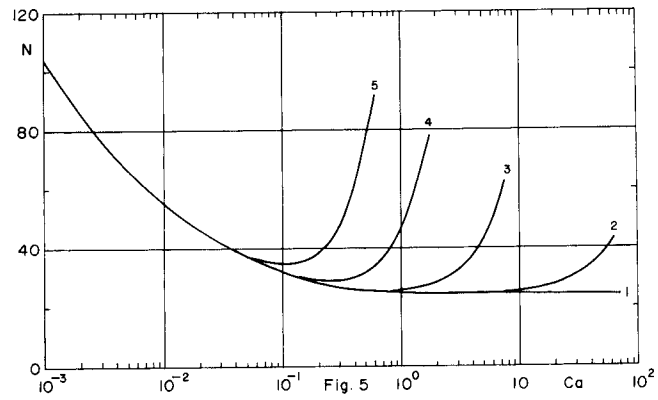

Fig. 5. The size of thin meniscus profiles: 1. $\gamma = 0$; 2. $\gamma = 0.06$; 3. $\gamma = 0.8$; 4. $\gamma = 5$; 5. $\gamma = 18.2$.

TABLE 1

$\gamma = 0.153$; $T = 0.720$; $Ca = 0.96$			$\gamma = 0.143$; $T = 0.769$; $Ca = 3.18$		
h	ξ	k	h	ξ	k
2.345	0.168	0.576	2.328	0.090	0.652
2.000	0.668	0.589	2.022	0.490	0.655
1.504	1.768	0.610	1.495	1.590	0.657
1.099	4.293	0.630	1.075	4.515	0.650
1.004	9.093	0.640	1.010	7.715	0.645
1.000	18.693	0.644	1.000	18.915	0.640
Experimental value $k = 0.602$			Experimental value $k = 0.562$		

TABLE 2

$\gamma = 0.130$; $T = 0.776$; $Ca = 6.21$			$\gamma = 0.141$; $T = 0.760$; $Ca = 10.5$		
h	ξ	k	h	ξ	k
2.347	0.056	0.671	2.312	0.123	0.659
2.032	0.456	0.666	2.017	0.523	0.641
1.507	1.556	0.652	1.497	1.723	0.610
1.061	4.981	0.630	1.046	5.948	0.577
1.009	8.181	0.622	1.008	9.148	0.569
1.000	19.381	0.615	1.000	21.948	0.560
Experimental value $k = 0.559$			Experimental value $k = 0.568$		

TABLE 3

$\gamma = 0.128$; $T = 0.664$; $Ca = 0.43$			$\gamma = 0.118$; $T = 0.731$; $Ca = 1.17$		
h	ξ	k	h	ξ	k
2.529	0.038	0.498	2.365	0.120	0.591
2.017	0.823	0.519	2.008	0.620	0.604
1.517	2.023	0.546	1.502	1.720	0.623
1.064	5.448	0.585	1.037	5.745	0.642
1.009	8.648	0.599	1.005	8.945	0.646
1.000	19.848	0.613	1.000	18.545	0.649
Experimental values $h = 1.2/3.0$; $k = 0.450$			Experimental values $h = 1.2/2.0$; $k = 0.588$		

TABLE 4

$\gamma = 0.113$; $T = 0.767$; $Ca = 2.75$			$\gamma = 0.122$; $T = 0.778$; $Ca = 5.66$		
h	ξ	k	h	ξ	k
2.317	0.107	0.647	2.370	0.028	0.671
2.014	0.507	0.652	2.049	0.428	0.668
1.490	1.607	0.658	1.511	1.528	0.657
1.088	4.232	0.655	1.049	5.253	0.637
1.004	9.032	0.650	1.007	8.453	0.630
1.000	18.532	0.648	1.000	19.628	0.623
Experimental values $h = 1.2/2.0$; $k = 0.714$			Experimental values $h = 1.1/3.0$; $k = 0.658$		

stable at very small Reynolds numbers for all wave disturbances of nonzero wave numbers. Therefore, we can conclude that the appearance of surface waves, which were not taken into our consideration, results in the failure of the solution at higher Reynolds numbers.

The literature contains extensive experimental data. Authors have measured the film thickness with a micrometer (Gutfinger and Tallmadge, 1965; Soroka and Tallmadge, 1971), with a capacitance technique (Spiers et al., 1974) and with light adsorption technique (Groenveld, 1970). These studies exhibit considerable scatter as can be seen on Figure 2. Spiers et al. (1974) has questioned the accuracy of the data of others, in part because of this scatter, and because it did not fit his data and curve. The effect of inertia γ seems to provide a better explanation, as the fit between the theoretical curves and the experimental data on Figure 2 seems excellent.

By comparison with the previous theories, Figure 3 illustrates the curves of the nonlinear theory, the gravitational theory of White and Tallmadge (1965), and the initial theory of Landau and Levich (1942).

Thin Meniscus Profiles

Using experimental results, Groenveld and Van Dortmund (1970) approximated the functional relationship between the intercept $(h - 1)$ and the distance above the bath ξ for thin meniscus profiles by

$$h = 1 + de^{-k\xi} \tag{26}$$

where $1/k$ is dimensionless thickness reduction distance, over which the excess thickness decreases $1/e$ times. Furthermore, Groenveld and Van Dortmond used a simplified two-dimensional linear approach, based on the approximation (26) to predict a value of k for the thin meniscus profiles. Their prediction, $k = 0.614$, was limited to high capillary numbers $Ca > 1$. Later, Tallmadge (1973) used the same approximation (26), based on his one-dimensional linear approach (1965) to predict the values of k for small capillary numbers $Ca \leq 10^{-1}$ as

TABLE 5

$\gamma = 0.118$; $T = 0.765$; $Ca = 11.9$			$\gamma = 0.119$; $T = 0.715$; $Ca = 23.9$		
h	ξ	k	h	ξ	k
2.338	0.085	0.667	2.437	0.056	0.628
2.034	0.485	0.648	2.029	0.656	0.563
1.502	1.685	0.616	1.501	2.156	0.505
1.043	6.010	0.581	1.083	6.181	0.467
1.007	9.210	0.574	1.005	12.581	0.453
1.000	22.010	0.564	1.000	26.975	0.446
Experimental values $h = 1.1/2.0$; $k = 0.606$			Experimental values $h = 1.2/2.0$; $k = 0.546$		

$$k = (3Ca)^{1/3}(1 - T^2)^{1/3}$$

The nonlinear theory (unlike the linear theories) gives a detailed shape to the thin meniscus profile which can be compared with these earlier predictions and with experimental data available. Equation (26) can be plotted as a straight line on a semilog plot. Figure 4 is a similar plot of the thin meniscus profiles obtained from the present calculations. A different slope results for each value of Ca, and the lines are not quite straight. In order to generalize, each profile can be represented by a parameter N which is a dimensionless version of L, the vertical distance from the stagnation point to the constant thickness region ($h \leq 1 + 10^{-7}$). Figure 5 illustrates the relationship

$$N = N(\gamma, Ca)$$

Experimentally, Groenveld and Van Dortmund (1970) obtained different values of k for different values of Ca. Since our results give a value k which changes with ξ as well as Ca, our ranges of values are compared with the reported numbers in Tables 1 and 2. For this purpose we measure ξ from the stagnation point (Figure 1). Thus, Equation (26) becomes

$$(h-1) = (2-T^2)\, e^{-k\xi} \qquad (27)$$

The agreement is quite reasonable.

Lee and Tallmadge (1972, 1973) reported in more detail the results of similar measurements made using a photographic technique. Their deep bath results for k varied with Ca but also varied with ξ as our theory predicts. Interestingly enough, Spiers and Wilkinson (1974) felt these results were in error because they did not agree with their one-dimensional solution. These experimental results may be compared more accurately with our theory because the range of thicknesses and the values of k are both available. Tables 3, 4, and 5 show that the agreement between theory and experiment is quite reasonable.

It has recently become a common practice to trust theory over experiment. We realize that even our theory has assumptions and that it must be confirmed by experiment or else fall. Therefore, it is very satisfying that there is agreement between our theory and the complete set of available data to the degree of precision of both.

ACKNOWLEDGMENT

The authors are grateful to the National Research Council of Canada for financial support.

NOTATION

a = meniscus thickness
a_0 = constant film thickness
b_i = coefficients of Galerkin's method expansion
Ca = capillary number $u_0\,\mu/\sigma$
g = acceleration of gravity
h = dimensionless meniscus thickness a/a_0
h_s = dimensionless thickness at stagnation point
k = shape parameter
L = extent of thin meniscus
N = dimensionless extent of thin meniscus L/a_0
n = ratio a_0/L
p = pressure of liquid
p_0 = static pressure of air
Q = liquid flux
Re = Reynolds number a_0u_0/ν
T = dimensionless film thickness $a_0(\rho g/\mu\, u_0)^{1/2}$
u = vertical velocity of liquid
u_0 = withdrawal speed
v = horizontal velocity of liquid
W_i = complete system of functions
x = vertical coordinate
y = horizontal coordinate

Greek Letters

γ = dimensionless parameter $\sigma(\nu^4 g)^{-1/3}/\rho$
μ = dynamic viscosity of liquid
ν = kinematic viscosity of liquid
ρ = density of liquid
σ = surface tension
ξ = nondimensional vertical coordinate x/a_0

LITERATURE CITED

Deryagin, B. V., and S. M. Levi, *Film Coating Theory*, Focall Press (1964).

Esmail, M. Nabil, and V. Ya. Shkadov, "Nonlinear Theory of Waves in a Viscous Liquid Layer," *Izv. Akad. Nauk SSSR, Mekh. Zhidk. i Gaza*, **4**, 54 (1971)., *Fluid Dynamics*, **6**, 599 (1973).

Esmail, M. Nabil, "Determination of Regions where Two-Phase Flow Wave Patterns Exist," *Teoret. Osnovy Khim. Tekhn.*, **7**, 1, 117 (1973).

Groenveld, P., "High Capillary Number Withdrawal from Viscous Newtonian Liquids by Flat Plates," *Chem. Eng. Sci.*, **25**, 33 (1970).

———, and R. A. Van Dortmund, "The Shape of the Air Interface during the Formation of Viscous Liquid Films by Withdrawal," *ibid.*, 1571.

Gutfinger, C., and J. A. Tallmadge, "Films of Non-Newtonian Fluids Adhering to Flat Plates," *AIChE J.*, **11**, No. 3, 403 (1965).

Landau, L., and B. Levich, *Acta Phys. URSS*, **17**, 41 (1942).

Lee, C. Y., and J. A. Tallmadge, "The Stagnation Point in Free Coating," *ibid.*, **19**, No. 4, 865 (1973).

———, "Description of Meniscus Profiles in Free Coating," *ibid.*, **18**, No. 5, 1077 (1972).

———, "Description of Meniscus Profiles in Free Coating II—Analytical Expressions," *ibid.*, **19**, No. 2, 403 (1973).

Shadov, V. Ya., "Wave Conditions in the Flow of a Thin Layer of a Viscous Liquid under the Action of Gravity," *Izv. Akad. Nauk SSSR, Mekh. Zhidk. i Gaza*, **1**, 43 (1967).

Soroka, A. J., and J. A. Tallmadge, "A Test of the Inertial Theory for Plate Withdrawal," *AIChE J.*, **17**, No. 2, 505 (1971).

Spiers, R. P., C. V. Subbaraman, and W. L. Wilkinson, "Free Coating of a Newtonian Liquid onto a Vertical Surface," *Chem. Eng. Sci.*, **29**, 389 (1974).

Spiers, R. P., and W. L. Wilkinson, "Uniqueness of Film Thickness and Meniscus Profiles in Vertical Withdrawal," *ibid.*, 1821.

Tallmadge, J. A., "The Shape of Dynamic Meniscus Profiles in Free Coating," *ibid.*, **28**, 311 (1973).

White, D. A., and J. A. Tallmadge, "Theory of Drag out of Liquids on Flate Plates," *ibid.*, **20**, 33 (1965).

Yih, C. S., "Stability of Liquid Flow down an Inclined Plane," *Phys. Fluids*, **6**, No. 3, 321 (1963).

Manuscript received Dec. 13, 1974; revision received and accepted May 13, 1975.

APPENDIX

According to the proposed condition $n << 1$, the expression (6) for the free surface curvature may be also simplified to yield

$$\frac{1}{R} \simeq \frac{db}{dx} = \frac{d^2a}{dx^2} \qquad (A1)$$

by neglecting terms estimated as $0(n^2)$. Integrating Equation (2) with respect to y, we get

$$p = \mu \frac{\partial v}{\partial y} + c\,(x)$$

where $c(x)$ is arbitrary function, which may be easily determined by using the boundary condition (17) and Equation (A1):

$$\mu\left(\frac{\partial v}{\partial y}\right)_a + c(x) = p_0 - \sigma\frac{d^2a}{dx^2} + 2\,\mu\left(\frac{\partial v}{\partial y}\right)_a$$

$$c(x) = p_0 - \sigma\frac{d^2a}{dx^2} + \mu\left(\frac{\partial v}{\partial y}\right)_a$$

By using the continuity Equation (15), the pressure p can be expressed as

$$p = p_0 - \mu\left[\frac{\partial u}{\partial x} + \left(\frac{\partial u}{\partial x}\right)_a\right] - \sigma\frac{d^2a}{dx^2} \qquad (A2)$$

Now, by using equations (18) and (A2), the terms of Equation (13) can be substituted by expressions including $U(x)$ and $a(x)$ as unknown functions along with the independent variables x, y:

$$u = 3\,U\left(-\frac{y}{a} + \frac{1}{2}\frac{y^2}{a^2}\right) + u_0$$

$$v = -3\frac{dU}{dx}\left(-\frac{y^2}{2a} + \frac{y^3}{6a^2}\right) - 3\,U\frac{da}{dx}\left(\frac{y^2}{2a^2} - \frac{y^3}{3a^3}\right)$$

$$\frac{\partial u}{\partial x} = 3\frac{dU}{dx}\left(-\frac{y}{a} + \frac{1}{2}\frac{y^2}{a^2}\right) + 3\,U\frac{da}{dx}\left(\frac{y}{a^2} - \frac{y^2}{a^3}\right)$$

$$\frac{\partial^2 u}{\partial x^2} = 3\frac{d^2U}{dx^2}\left(-\frac{y}{a}+\frac{1}{2}\frac{y^2}{a^2}\right)+6\frac{dU}{dx}\frac{da}{dx}\left(\frac{y}{a^2}-\frac{y^2}{a^3}\right)$$
$$+3U\frac{d^2a}{dx^2}\left(\frac{y}{a^2}-\frac{y^2}{a^3}\right)+3U\left(\frac{da}{dx}\right)^2\left(-\frac{2y}{a^3}+\frac{3y^2}{a^4}\right)$$

$$\frac{\partial u}{\partial y} = 3\,U\left(-\frac{1}{a}+\frac{y}{a^2}\right)$$

$$\frac{\partial^2 u}{\partial y^2} = 3\,U/a^2$$

$$\frac{\partial p}{\partial x} = -\mu\left[\frac{\partial^2 u}{\partial x^2}+\frac{\partial}{\partial x}\left(\frac{\partial u}{\partial x}\right)_a\right]-\sigma\frac{d^3a}{dx^3}$$

Substituting the last expressions in Equation (13), and integrating with respect to y from zero to a, we get

$$\rho\left(\frac{9}{10}a\,U\frac{dU}{dx}-\frac{3}{10}U^2\frac{da}{dx}-a\,u_0\frac{dU}{dx}+\frac{u_0}{2}U\frac{da}{dx}\right)$$
$$=\sigma a\frac{d^3a}{dx^3}-\frac{7}{2}\mu a\frac{d^2U}{dx^2}+2\mu\frac{da}{dx}\frac{dU}{dx}+3\mu\frac{U}{a}-\rho\,ga$$
$$+\mu U\frac{d^2a}{dx^2} \quad \text{(A3)}$$

By using Equation (20), the constant flux condition along the meniscus can be expressed as

$$Q=\int_0^a u\,dy = a(x)\;[u_0-U(x)]$$

By using the last equation, the function $U(x)$ can be substituted in Equation (A3) by the function $a(x)$, and we get

$$\rho\left(\frac{u_0^2}{5}a^2\frac{da}{dx}-\frac{6}{5}Q^2\frac{da}{dx}\right)=\sigma a^3\frac{d^3a}{dx^3}+\left(\mu u_0 a^2\right.$$
$$\left.-\frac{9}{2}\mu Qa\right)\frac{d^2a}{dx^2}+9\mu Q\left(\frac{da}{dx}\right)^2+3\mu u_0 a-3\mu Q-\rho g a^3 \quad \text{(A4)}$$

By introducing the dimensionless variables

$$h=\frac{a}{a_0} \qquad \xi=\frac{x}{a_0}$$

Equation (A4) reduces to Equation (21).

Numerical Treatment of Laminar Flow in Helically Coiled Tubes of Square Cross Section

Part I. Stationary Helically Coiled Tubes

B. JOSEPH
E. P. SMITH
and
R. J. ADLER

Chemical Engineering Department
Case Institute of Technology
Case Western Reserve University
Cleveland, Ohio 44106

Numerical solutions of steady laminar flow in helically coiled tubes of square cross section for Dean numbers from 0.8 to 307.8 reveal two regimes of secondary flow. Up to Dean numbers of 100, the expected secondary flow pattern appears with twin counterrotating vortices. Above Dean numbers of 100, a new secondary flow regime, reported here for the first time, appears with four vortices. Flow visualization and pressure drop experiments confirm the transition.

SCOPE

When fluid flows through a helically coiled tube, centrifugal forces cause secondary flows, that is, currents in the cross-sectional plane. The fluid near the center of the tube, because it has the maximum downstream velocity, experiences the maximum centrifugal force and is thrown outward. Replacement fluid flows inward along the walls. A secondary flow pattern consisting of twin counterrotating vortices has been reported in all previous studies.

Helically coiled tubes often appear in process applications. Useful characteristics include, in addition to compactness, high rates of heat and mass transfer, enhanced cross-sectional mixing, low axial dispersion and an extended laminar flow regime—the transition from laminar to turbulent flow occurs at Reynolds numbers of 4,000 to 6,000 for typical geometries.

Most prior studies on helically coiled tubes have been for round cross sections. The only study of rectangular cross sections is an analytical solution limited to very low flow rates. However, rectangular cross sections arise in

Correspondence concerning this paper should be addressed to R. J. Adler.